Nutritional exchange between reef-building corals and algal endosymbionts buffers the energetic demand of larval development and metamorphosis

Ariana S. Huffmyer* [1,2], Kevin H. Wong [1, 3], Danielle M. Becker [1], Emma Strand [1], Tali Mass [4], Hollie M. Putnam [1]

1. Department of Biological Sciences, University of Rhode Island, Kingston RI 02881 USA
2. School of Aquatic and Fishery Sciences, University of Washington, Seattle WA 98105 USA
3. Rosenstiel School of Marine and Atmospheric Science, Department of Marine Biology and Ecology, University of Miami, Miami FL 33149 USA
4. Department of Marine Biology, The Leon H. Charney School of Marine Sciences, University of Haifa, 3498838, Mt. Carmel, Haifa, Israel

*Corresponding author: Ariana S. Huffmyer; ashuffmyer@gmail.com

Keywords: Montipora capitata, Symbiodiniaceae, metabolomics, transcriptomics, larvae

Running Title: Developmental transitions in coral-symbiont nutritional exchange

Abstract

Anthropogenic climate change threatens the persistence of coral reefs by impacting reproduction and accelerating coral loss. Adult corals depend on nutritional exchange with their endosymbiotic algae (Symbiodiniaceae) to fulfill their energetic demands. However, the mechanisms underlying the onset of this exchange during early life stages and how it contributes to developmental energy demands are unclear. We conducted an integrative analysis of metabolism across developmental stages in *Montipora capitata*, a vertically transmitting coral (Symbiodiniaceae are passed from parent to offspring) in Hawai□i. We applied physiological (metabolism and symbiont density) and multi-omic (metabolomics, transcriptomics, and microbial amplicon sequencing) approaches over 13 time points between 1-255 hours post-fertilization from eggs to settled recruits. Energetic demand (respiration) increased as embryos developed into larvae and progressed through metamorphosis. Symbiont photosynthetic capacity (photosynthesis and cell density) increased across ontogeny, demonstrating potential for symbiont-derived nutrition to fuel coral development and growth. Indeed, gene expression and metabolomic analyses revealed that symbiont-derived nutrition is metabolized starting in the motile larval stage with increasing utilization during metamorphosis and following settlement. Specifically, gene and metabolic pathways associated with organic compound transport and glucose and fatty acid metabolism were enriched and there was expanded use of carbohydrate and lipid metabolism in metamorphosed polyps and recruits. Larvae also demonstrate increased cellular processes to maintain nutrient balance between host and symbiont and regulate symbiont populations through expression of genes that regulate nitrogen assimilation and response to reactive oxygen species. Collectively, our multi-omic

characterization reveals that symbiont-derived nutrition becomes increasingly important to buffer energetic demands required for coral settlement. In environmentally stressful conditions, early life stages of vertically transmitting species may be increasingly vulnerable to the loss of symbiont-derived nutrition. Therefore, early interventions to reduce symbiotic stress during sensitive developmental stages could enhance coral reef recruitment and recovery as climate change intensifies.

Introduction

Symbiotic relationships between animals and microbial organisms enable survival in nutritionally challenging environments (1). The function and structure of one of the most ecologically and economically important ecosystems on Earth, coral reefs, is driven by the productivity of marine symbioses. The nutritional symbiosis between reef-building corals and endosymbiotic algae in the family Symbiodiniaceae (2) can provide >100% of the coral's daily metabolic demands through translocated organic carbon generated through symbiont photosynthesis (3, 4). In return, metabolic waste from the coral host, including nitrogen and inorganic carbon, is provided to Symbiodiniaceae to support their cellular metabolism and population growth (5, 6). The energy-enhancing nutrient exchange between Symbiodiniaceae and corals, as well as their diverse bacterial and archaeal microbiome (7), enables calcium carbonate production and thus the formation of the 3D skeletal structure that provides a habitat for high ecosystem biodiversity (8) and invaluable goods and services (9). However, this delicate symbiosis is susceptible to destabilization by environmental stress. Rising sea surface temperatures and acute marine heat waves cause coral bleaching, or the dysbiosis and loss of photosynthetic pigments and/or symbiont cells, and their carbon surplus from the coral (10), which can, and often does, culminate in mortality at reef-wide levels (11). Increasingly, the stability and persistence of the nutritional relationship between corals, their algal endosymbionts, and symbiotic microbes is critical for the continued survival of reefs and the maintenance of essential ecosystem services that people in tropical coastal communities rely on.

Globally, half of the live coral cover has been lost since the 1950s (12), significantly increasing the importance of coral reproduction and recruitment to replenish and maintain reef ecosystems. Corals have complex and biphasic life cycles, in which sessile adults produce gametes that are internally or externally fertilized and develop into swimming larvae that then undergo metamorphosis into the sessile polyp recruit stage and grow into mature colonies attached to the benthos (13). Survivorship from fertilization to recruitment represents the primary bottleneck for marine larvae (14), due to environmental impacts on fertilization, larval dispersal and behavior, predation, substrate suitability, and post-settlement survival (13). Key among the myriad challenges facing these sensitive life stages is the energetic requirement for successful development, metamorphosis, and calcification (15). To buffer these energetic challenges, corals form associations with Symbiodiniaceae either immediately through vertical transmission (i.e., symbionts are provisioned to the eggs), or within days to weeks of release and/or settlement through the process of horizontal transmission (i.e., symbionts are acquired from the environment) (16). Initiation of symbiosis is a topic of intense study (17), but the timing of productive nutritional exchange and the contribution of nutritional exchange to energy

demand in early life history remains less well understood despite its increasing importance to reef persistence and recovery (18).

The establishment of nutritional symbioses in early life history has direct implications for coral survival. Without symbiotic nutritional sources, coral embryos and larvae initially rely on limited endogenous lipid reserves in the forms of phospholipids (primarily for use in cell membranes), wax esters (most abundant class available as fatty acid reserves for metabolic oxidation), and triacylglycerols (storage lipids that can be rapidly metabolized) (19). Furthermore, there are conflicting findings on the capacity of the coral-algal symbiosis to contribute substantially to the energetic demands of early life stages. For example, high-performance thin-layer chromatography lipid analysis in aposymbiotic larvae indicates a decline in wax ester abundance as larvae age, with a strong reliance on parentally provisioned fatty acids for energetic fuel (20). In symbiotic larvae, this demand for energy reserves can be supplemented by symbiotic nutrition, observed as carbon translocation (21) and reduced rates of lipid depletion under light conditions (22). In contrast, stable isotope pulse-chase and nanoscale secondary ion mass spectrometry (NanoSIMS) imaging in symbiotic larvae indicate that nutritional exchange is possible, but substantially lower relative to levels of exchange at the adult stage (23), highlighting the need for ontogenetic and mechanistic studies to resolve the role of symbiotic nutrition in contributing to recruitment costs. This is especially critical as the heavy reliance on nutritional exchange during early life history can increase susceptibility to environmental stressors, such as light driven increases in cellular damage due to the presence of symbionts (24). As thermal stress increases with climate change, bleaching and symbiotic disruption will further destabilize nutritional exchange and worsen recruitment bottlenecks. Therefore, to understand how symbiont-derived nutrition affects coral recruitment under ocean warming, it is important to quantify metabolism and assess evidence for various mechanisms of nutrient exchange across life stages from gametes to calcifying juveniles. The quantification of biological response at molecular and metabolomic levels provides the capacity to detect the shift from reliance on parental provisioning of lipids (e.g., metabolism of wax esters and storage lipids) to nutrition provided by symbionts (e.g., glucose metabolism and transmembrane transporters).

Considering the critical need to increase our understanding of the sensitive coral symbiosis and energetic demands of recruitment, we characterized ontogenetic shifts in metabolism and symbiotic exchange of the vertically transmitting coral, *Montipora capitata* using a cross-scale approach integrating physiological, transcriptomic, metabolomic, and microbiome data (Fig 1AB). We found that symbiotic nutritional exchange contributes to coral metabolism as early as the swimming larval stages and increases during the energetically demanding processes of metamorphosis and settlement. Molecular and metabolomic evidence demonstrates that symbiont-derived nutrition is increasingly metabolized throughout ontogeny, starting in the larval stages, and corresponds with host regulation of metabolic byproducts and regulating symbiont population growth. Following metamorphosis, there is increased utilization of photosynthetic products to buffer the energetic demands of settlement. This comprehensive characterization of early life history metabolism demonstrates that energy demands can be buffered by symbiotic nutritional exchange and identifies larvae and new recruits as the ontogenetic windows that are particularly vulnerable to symbiotic stress because of climate change.

Results and Discussion

A. Energetic demands of development and metamorphosis can be buffered by endosymbiont productivity

Progressing through development is an energetically demanding process (25, 26), and it has been debated whether symbiotic nutritional exchange meaningfully contributes to these requirements (23). To address this, we tracked growth, respiratory demand, and symbiont photosynthesis in early coral life stages (65-231 hours post fertilization, hpf) (Fig 1AB). First, there were significant changes in individual size across development (Kruskal-Wallis, $\chi^2(8,512)=225.33$, $P<0.001$; Fig 2A). Specifically, embryo size decreased 41% as development progressed from egg (1 hpf) through larval stages as corals went through size contraction associated with the transition from the late gastrula (65 hpf) to planula (93 hpf) stages (Fig 2A). Size then increased, reaching maximum at 231 hpf (142% growth relative to egg size; Fig 2A) in larvae and metamorphosed polyps.

Larval growth from 93 to 231 hpf corresponded with elevated respiratory demand (58% growth from 93 to 231 hpf). In particular, respiration rates increased across ontogeny (one-way ANOVA; $F(5,91)=49.91$, $P<0.001$; Fig 2B) in response to developmental costs associated with tissue growth and differentiation as well as increases in swimming behavior at the larval stage (27). Further, respiration rates were significantly higher in metamorphosed polyps as compared to swimming larvae at the same time point (82% higher at 183 hpf, post hoc $p<0.001$; 151% higher at 231 hpf, post hoc $p<0.001$). This large increase in respiratory demand upon metamorphosis is consistent with observations in Pocilloporid recruits of an 83% increase in post-metamorphosis respiration relative to larvae (28) and emphasizes the high energetic cost of rearrangement of the body plan (29) and initiation of biomineralization (30, 31). The ontogenetic increases in respiratory demand necessitate the acquisition of additional or external nutritional resources beyond stored energy reserves (19). Therefore, symbiont-derived nutrition is essential to support successful development and ultimately survival, even if it is available at lower amounts than in adults (23).

Our quantification of symbiont response supports the hypothesis that symbiont-derived nutrition ramps up quickly and significantly post-fertilization, which can assist in supporting larval growth and development. Photosynthesis rates increased 77% from earliest (65 hpf) to latest (231 hpf polyp) stages, with the largest increase occurring between 93 and 183 hpf (Fig 2C; one-way ANOVA, $F(5,91)=9.36$, $P<0.001$). The rapidly increased photosynthetic rates coupled with high symbiont population growth of 142% (between 93 and 231 hpf) during larval and metamorphosed stages (Fig 2E; ANOVA, SS=1.02e8, $F(9,30)=25.06$, $P<0.001$) indicate nutritional contribution from the symbionts through the production of fixed carbon products (4, 32), particularly after 93 hpf in *M. capitata*. Despite increasing photosynthesis, however, energetic demand soars during metamorphosis, reducing the photosynthesis : respiration ratio significantly (Fig 2D; one-way ANOVA, $F(5,91)=11.3$, $P<0.001$) at 183 hpf (P:R=1.19 ± 0.16). This observation further demonstrates that reduction of symbiont-derived nutrition driven by environmental stress, such as increased temperatures (32, 33) would further exacerbate the energetic vulnerability of coral recruitment (18, 34, 35).

B. Symbiotic community composition remains stable alongside increases in bacterial community diversity

Our results indicate no evidence of winnowing or selection of symbiont partners with ontogeny in *M. capitata.* The increased photosynthetic capacity with ontogeny is driven by the growth and physiology of a stable, mixed *Cladocopium* spp. and *Durusdinium glynnii* symbiont population. In previous studies, shifts in symbiont community composition in adult *M. capitata* have impacted holobiont performance (36, 37). A mixture of *Cladocopium* sp. and *Durusdinium* sp. is characteristic of this species in Kāne□ohe Bay, Hawai□i (36, 38). Our samples contained a majority (55.9±0.8%) of *Cladocopium* sp. (ITS2 Profile C31.C17d.C21.C21ac.C31a; (39)) and minority (44.1±0.8%) of *Durusdinium glynnii* (ITS2 Profile D1.D4.D6.D1ab.D17d; (40)) (Fig S1). Neither the alpha diversity of our Symbiodiniaceae ITS2 profiles, or Defining Intragenomic Variant (DIVs (35)) (Kruskal-Wallis, $\chi^2(9,28)=9.541$, $P=0.389$; Fig S2), nor the symbiont community similarity (PERMANOVA, SS=0.360, $R^2=0.261$, $F(9,28)=1.098$, $P=0.217$) differed by timepoint, demonstrating stable symbiont communities in early life history (Fig S1) under ambient conditions. However, as environmental conditions continue to change (e.g., chronic temperature stress and increase in acute heat waves), the thermal tolerance of *D. glynnii* previously documented in adult *M. capitata* (41, 42) could manifest in a shift to a greater abundance of *D. glynnii* than *Cladocopium sp.* provisioned to offspring (43). As *D. glynnii* translocates lower amounts of photosynthates than *Cladocopium sp.* in *M. capitata* (32), this could result in detrimental impacts on nutritional availability for offspring in the future.

Coral holobiont performance is driven by nutritional cycling between the various partners, however, the nutritional linkages between corals and bacterial communities (44, 45) are not fully clear at these early life stages. Bacterial communities play important roles in nutritional cycling (46–48) and acquisition of micronutrients (49) and can act as nutritional mediators between host and symbiont (45, 50). For example, larvae of the brooding coral *Pocillopora acuta* transfer bacterially derived nitrogen to their symbiont populations (50). Given that we documented shifts in photosynthetic capacity and symbiont population growth, we further investigated bacterial community composition and stability in *M. capitata* early life stages. In contrast to the observed stability in Symbiodiniaceae communities, bacterial communities varied significantly across development (PERMANOVA, SS=4.879, $R^2=0.643$, $F(7,17)=4.378$, $P=0.001$), and notably, alpha diversity peaked during metamorphosis and recruitment (one-way ANOVA; Shannon: SS=20.247, $F(7,17)=22.31$, $P<0.001$; Inverse Simpson: SS=1.69e4, $F(7,17)=17.46$, $P<0.001$) (Fig S2AB), at the same stages as maximal energy demand. This enhanced diversity of microbiome communities during metamorphosis and settlement could also be due to interactions with the substrate and the production of antimicrobial compounds to defend against benthic bacteria (13, 51). Our observation of developmental succession and shifts in bacterial communities is supported by previous observations in *Coelastrea aspera* that showed bacterial diversity increased from recruit (<6 cm colony diameter) to adult colonies (>28 cm in colony diameter) (52). Due to lower than anticipated sequencing depth in our samples, we constrained our analysis at the higher taxonomic levels of genus or above. Specifically, we found that Alteromonadaceae (*Alteromonas* sp.), *Vibrio* sp., and Pseudoalteromonadaceae (*Psychrosphaera* sp.) peak early in

development followed by Oceanospiriliaceae (unclassified) increasing in larval stages (Fig S2CD). In late development (larvae through recruits), the relative abundance of Rhodobacteraceae and Flavobacteriaceae increases (Fig S2CD). These taxa play important roles in carbon (53), nitrogen (50), sulfur (e.g., DMSP/DMS; (54)), and micronutrient cycling (49) along with the production of antimicrobial compounds (55). Therefore, we hypothesize that our observations of an increase in bacterial diversity could confer increased nutritional functional diversity and capacity for nutrient cycling as corals age (56, 57). To test this hypothesis, quantitative measures of nutrient cycling between bacterial communities and the coral host should be completed in future studies with approaches such as metatranscriptomics, DNA-stable isotope probing (e.g., DNA-SIP), as well as metabolomic stable isotope probing and microscopy techniques (e.g., NanoSIMS) applied to early life stages (58).

C. Metabolism of symbiont-derived nutrition becomes increasingly important across coral development to supplement reserves and meet energetic demand

In concert with our documentation of the positive relationships between photosynthetic rates, respiratory demand, symbiont density, and bacterial diversity with age, our molecular and metabolomic data strongly support an increased host-symbiont nutritional exchange across ontogeny. We quantified ontogenetic shifts in gene expression and metabolomics through TagSeq (59) and liquid chromatography–mass spectrometry (LCMS) metabolomics (*sensu;* (60)), respectively, and assessed these data via weighted co-expression network analyses (WCNA; (61). There were strong gene expression (PERMANOVA; SS=3.18e5, R^2=0.751, F(9,28)=9.362, *P*=0.001) and metabolic (PERMANOVA; SS=5.39e3, R^2=0.644, F(12,34)=5.122, *P*=0.001) shifts across development (Fig S3), which when analyzed at the functional level lend further support for symbiotic nutritional exchange across development and the mechanisms by which this occurs.

Three ontogenetic patterns emerged from independent network analyses of both gene expression (Fig 3AB) and metabolite quantification (Fig 4AB): *Decreasing*), a peak in eggs and embryos and subsequent decrease across development; *Mid*) an increase in mid development, peaking in larval stages; and *Increasing*) an increase across development, peaking in late larvae, metamorphosed polyp, and recruit stages. By examining the functional enrichment within each of these three patterns (GOSeq Biological Processes ontology and MetaboAnalyst; see details in Supplementary Methods; Fig S4, Fig S5) for key areas of interest for understanding symbiotic and metabolic shifts across development, including carbohydrate metabolism (“carbohydrate”), lipid metabolism (“lipid”, “fatty acid”), and communication and transport ("regulation of cell communication", "transmembrane", "organic substance transport", "antioxidant", "oxygen") (Fig 3CDE; Fig 4CD) we are able to identify the rise and fall of key indicators of symbiotic nutritional exchange. For specific indicators, we additionally tracked a subset of genes with key GO terms including “carbohydrate metabolism”, “glucose metabolism”, “lipid metabolism”, and “oxidative stress” (Fig 5). We also tracked metabolite pool sizes of compounds involved in key pathways such as glycolysis, the tricarboxylic acid cycle, ammonium metabolism, and energy cofactor and carrier metabolism (Fig 6) across all sampled developmental stages. We discuss our findings in the areas of: i) the use of parentally-derived metabolic building blocks; ii) initiation of nutritional exchange and symbiosis regulation; and iii)

integration of symbiotic metabolism to meet energetic demand for metamorphosis and calcification.

i. Early development: The use of parentally derived metabolic building blocks

Parentally provisioned transcripts and macromolecules provide the molecular capacity and energy required for rapid cell proliferation and growth during coral embryonic development (62). In early development, embryos undergo a reorganization of tissues and cellular structures, gastrulation and differentiation of germ layers, and rapid cell proliferation (63–65). These processes require parental transcripts, structural molecules, and metabolic building blocks (e.g., glycogen, amino acids, lipids) and capacity for cell signaling and transport that are provisioned to eggs from the parent (66–68). Our results demonstrate that parentally-provisioned reserves are utilized as the primary source of energy in early development in *Montipora capitata* (<65 hpf).

Use of parental reserves is indicated in our datasets by the enrichment of genes involved in the metabolism of amino sugars and simple carbohydrates (Fig 3C) and lipids (lipid catabolic process) in early development. Corroborating results from metabolomics analysis show that there is an increase in metabolites that result from the catabolism of stored carbohydrates (monosaccharides, tricarboxylic cycle acids) and derivatives (glycosyl compounds) (Fig 4C). Previous work observed enrichment of lipid catabolic process and monosaccharide metabolic process genes in the aposymbiotic blastula/prawn chip stage (12 hpf) of *Acropora digitifera (64)*, which provides further evidence that the metabolic processes observed in *M. capitata* embryos result from metabolism of parentally provisioned reserves and not symbiont-derived nutrition. Further, there is limited evidence for metabolism of symbiont-derived nutrition produced by symbiont populations in embryos in early development. Specifically, the expression of genes involved in symbiont-derived nutrition such as carbohydrate, glucose, lipid, and fatty acid metabolism, which are the main components of photosynthates (69, 70), were lowest in egg and embryo stages as compared to later developmental stages ($p<0.001$; Table S1; Fig 5). There was an accumulation of glucose and glycolysis intermediate pools (glucose-6-phosphate), along with lower pools of pyruvate, a product of glycolysis, (Fig 6A) which suggests lower carbon metabolism through glycolysis in early development as compared to later stages. Another indication of low glycolytic metabolism in early development is the accumulation of oxidized forms of energetic cofactors, including NAD+ (Fig 6F). NAD+ is an important cofactor in the glycolysis pathway and glycolysis results in the reduction of NAD+ to NADH (71). Therefore, higher pools of NAD+ indicate low glycolytic metabolism in eggs and embryos. These lines of evidence suggest that metabolism of actively produced photosynthates is low in early development, and rather, embryos rely on parentally provisioned resources for metabolic needs.

Further evidence that early development is supported by parentally provisioned molecules and transcripts is the activation of metabolic pathways that generate important metabolic building blocks and cellular functions. Specifically, there was enrichment in immune and apoptosis regulation systems (regulation of kappaB, NF-kappaB, and hippo signaling), cell signaling (G-protein coupled receptor regulation, signal transduction regulation, steroid metabolism), and transport (organic substance and amino acid transport and ion transport) (Fig

3DE) in early development. A previous study in the same species found that functions related to metabolism, biosynthesis, transport, and signaling were enriched in maternally provisioned transcripts (prior to the first wave of transition to zygotic mRNA at ~ 4 hpf) (62), suggesting that these functions are a product of maternal mRNA provisioning in our samples.

Since carbon metabolism through glycolysis is low in early development, ATP is likely primarily produced by metabolism of provisioned parental resources. This can be seen in the rapid increase in ATP from 1 to 5 hpf ($p<0.001$; Table S1) (Fig 6E), indicating that metabolism of energy sources packaged in eggs from the parent is producing cellular energy for rapid proliferation and differentiation (68). A complementary line of evidence shows that there was a sharp significant decrease in glycerol-3-phosphate between 1 and 5 hpf, (one-way ANOVA, $SS=0.099$, $F(1,6)=106$, $p<0.001$) (Fig S6). This metabolite is produced from the catabolism of glycerol, which is an important component of translocated photosynthates from symbiont to host (69). Because spawning occurs at night when symbiont photosynthesis is not active and therefore not actively producing photosynthates for embryonic metabolism from 1-5 hpf, this data supports the prior finding that photosynthates can be packaged and stored in the eggs from the parents (68). Indeed, intermediate metabolites of the tricarboxylic acid (TCA) cycle including succinate, fumarate, isocitrate, and citrate exhibit a sharp decrease in pool size between 1 and 5 hpf (Fig 6B), indicating an increased rate of this pathway (i.e., increased intermediate turnover and usage) for producing ATP for developing embryos from stored reserves (72). Our results are also supported by previous observations that aposymbiotic larvae utilize similar lipid and simple carbohydrate metabolic processes to fuel early development that were provisioned by the parents (73) in the absence of symbiont communities. Therefore, metabolic demand during early embryonic development (i.e., <65 hpf in this study) can be sustained without active translocation and nutritional exchange between corals and algal symbionts.

These results from gene expression and metabolomic data demonstrate that the energy demand of development and metabolism during embryonic stages up to 65 hpf in *M. capitata* is driven by parentally-provisioned reserves, with limited evidence for symbiotic nutritional exchange. Because parental provisioning is critical for early embryonic development, environmental stressors that compromise adult coral energy for gamete provisioning (68) may compromise the energetic resources available to early life stages, especially during reproductive events following mass bleaching events (74).

ii. Mid-development: Initiation of nutritional exchange and symbioses regulation

Within the patterns of genes and metabolites that peak in the middle of *M. capitata* development, molecular (Fig 3) and metabolomic evidence (Fig 4) supports metabolism of symbiont-derived nutrition and establishment of symbiotic exchange. In the coral-Symbiodiniaceae symbiosis, carbohydrates, amino acids, fatty acids, and other compounds are produced through photosynthesis and translocated to the host (75–78). Glucose is a major metabolite involved in nutritional transfer (70) and in this study, is a key metabolite utilized by the host at the onset of host-symbiont nutritional exchange. In larval stages, genes involved in glucose, hexose, and monosaccharide metabolic processes (Fig 3C) are enriched along with monosaccharides, disaccharides, and metabolites involved in carbohydrate metabolism (Fig

4CD). Indeed, when viewed across development, there is an increase in the expression of genes involved in carbohydrate and glucose metabolism (Fig 5AB). Metabolomic evidence demonstrates that the rate of glycolysis increases during this developmental window. Specifically, the pool size of glucose-6-phosphate, a glycolysis intermediate, decreases while both glucose and a product, pyruvate, increase ($p<0.001$; Table S1) (Fig 6A). Concurrently, there is a reduction in the oxidized cofactor NAD+, which is reduced to NADH in glycolysis (71) and provides further evidence that central carbon metabolism increases during this developmental window ($p<0.001$; Table S1) (Fig 6F). These results suggest that the rate of glycolysis and the available pool of glucose to metabolize through glycolysis are increasing in mid-development and, therefore, that symbiotic nutritional exchange and metabolism of this energy source is increasingly utilized in larval stages. To facilitate the translocation and metabolism of carbohydrates, carbohydrate derivative transport and carboxylic acid and organic acid transmembrane transport are active in larval stages (Fig 2E) and glucose transporter genes are expressed consistently across development ($p=0.682$; Table S1) (Fig 5C). This utilization of carbohydrates in larval stages supports prior observations that symbiotic larvae use stored reserves at lower rates due to the added energy supplement from symbiont photosynthates (22). Our results show that carbohydrate and glucose metabolism concurrent with increased symbiont density and photosynthetic rates demonstrates that these larvae have the molecular machinery and metabolic capacity to utilize photosynthates.

Fatty acids are energy-rich compounds that are also largely acquired from the symbiont (e.g., saturated and polyunsaturated fatty acids, docosahexaenoic acid, arachidonic acid, and palmitic acid) (79, 80). In adult corals, fatty acids translocated from the symbionts can be directly metabolized through beta-oxidation in the epidermis, and, simultaneously, excess translocated glucose can be used to synthesize fatty acids in gastrodermis cells and subsequently stored as neutral lipids or wax esters for later use (81). Our data indicate that both fatty acid oxidation and lipid biosynthesis from fatty acids are occurring in larval stages. First, there was enrichment in fatty acid oxidation (Fig 3D) along with metabolomic enrichment of fatty acids and conjugates and short-chain acids and derivatives (Fig 4C), suggesting that fatty acids from the symbiont are translocated, evidenced by enrichment of organic acid transmembrane transport (Fig 3DE), and directly metabolized. Further, gene expression of genes involved in fatty acid metabolism increase and are highest in late larval and metamorphosed polyp stages ($p<0.001$; Table S1) (Fig 5F). Second, genes involved in fatty acid derivative biosynthesis and positive regulation of lipid biosynthetic processes were enriched, demonstrating that the host is also synthesizing fatty acids from carbohydrate sources and building stored reserves (Fig 3D). Throughout development, genes involved in lipid metabolism and regulation and lipid catabolism are enriched (Fig 3D) and peak in larval stages ($p<0.001$; Table S1) (Fig 5D), indicating continual utilization of stored lipid reserves to support developmental costs (20, 22). Because the metabolism of one class of storage lipids, triacylglycerides, does not emerge until late development (described below), lipid metabolism in mid-development is most likely from the catabolism of wax ester stores, which is the largest lipid fraction in coral tissues and the primary parentally provisioned energy source in larvae (19, 20). As the contribution of photosynthates increases, translocated fatty acids may be utilized to rebuild depleted wax ester stores through time. Our understanding of ontogenetic shifts in lipid translocation and utilization would be

improved by the characterization of lipid classes and fatty acid profiles (e.g., (82)) across life stages in vertically transmitting species.

The productivity and stability of the symbiotic relationship is highly dependent on nitrogen cycling (47). Active host nitrogen limitation to the symbionts can enhance the translocation of excess photosynthetically fixed carbon back to the host and manage symbiont population growth (5, 47, 83). Notably, our data demonstrate that nitrogen cycling occurs during the larval period through enrichment in alanine, aspartate, and glutamate metabolic pathways in larvae (Fig 4D) and an increase in genes (Fig 5G) and metabolites (Fig 6C) involved in ammonium metabolism ($p<0.001$; Table S1). Specifically, ammonium metabolism through the glutamine synthase/glutamine oxoglutarate aminotransferase pathways (GS/GOGAT) play an important role in nitrogen assimilation and supporting growth and function of nitrogen-limited symbionts (6, 84–86). Through these pathways, ammonium is assimilated into amino acids through sequential action of glutamine synthase (produces glutamine from glutamate and ammonium; GS) and glutamine oxoglutarate aminotransferase (produces two molecules of glutamate from glutamine and α-ketoglutarate; GOGAT), which generates amino acids that can be used for a wide variety of cellular functions and metabolism (85, 87, 88). Glutamate can also be produced from α-ketoglutarate and ammonium through the anabolic activity of glutamate dehydrogenase (GDH) pathway (85, 86). Although the coral host has the capacity to acquire ammonium through these pathways (85, 89), the symbiont is capable of up taking and fixing 14-23 times more ammonium than the host (85).

Previous work suggests that host assimilation of ammonium results in less free ammonium available to the symbiont (86, 90), which limits symbiont population growth and favors the translocation of excess photosynthetically fixed carbon (e.g., glucose) back to the host (75, 91). Indeed, we found that across development there was a steady increase in glutamine pools relative to glutamate across development ($p<0.001$; Table S1; Fig 6C) and increasing expression of ammonium metabolism host genes ($p<0.001$; Table S1; Fig 5G), indicating increasing ammonium assimilation through the GS pathway (92). Therefore, ammonium assimilation in early development may be a mechanism for nitrogen limitation of the symbiont population to facilitate translocation of photosynthates for host metabolism in larval stages. This hypothesis is supported by previous work in symbiotic anemones demonstrating that the presence of symbiont-derived glucose activates ammonium assimilation pathways, which does not occur in aposymbiotic individuals (81, 89). This suggests that the establishment of symbiotic nutritional exchange is closely tied to nitrogen cycling in the holobiont and is a product of complex feedback loops (86). Ontogenetic shifts in nitrogen fixation and ammonium assimilation should be further documented through nitrogen tracing studies (88) to fully elucidate the role of nitrogen cycling on establishment of nutritional exchange in early life history.

The expression of bicarbonate transporters in larval stages ($p<0.001$; Table S1) (Fig 5E) is another indicator that nutritional exchange is occurring and that the host is providing symbionts with inorganic carbon required for photosynthesis (6). The enhancement of photosynthesis and symbiont growth is not without its dangers from temperature and irradiance driven production of reactive oxygen species (ROS) (24, 93, 94). As metabolic activity increases to fuel developmental demands, larvae must employ cellular stress and management techniques to maintain a stable symbiosis (95, 96). We observed that larvae had enriched gene

expression for regulation and metabolism of ROS and immune and stress response signaling (terpenoid and sphingolipid metabolism, protein kinase B signaling) (Fig 2E) (17, 91, 95, 97). Further, expression of genes involved in oxidative stress were elevated in larval stages and peaked during metamorphosis ($p<0.001$; Table S1) (Fig 5H). Methionine sulfoxide, an ROS scavenging metabolite associated with heat stress in corals (60), increased across development with a peak in larval stages and a second peak later in recruit stages ($p<0.001$; Table S1) (Fig 6D).

Our examination of gene expression and metabolite patterns peaking at mid-development demonstrate that the metabolic transition towards increased utilization of symbiont-derived nutrition begins in larval stages in *M. capitata*. Symbiotic nutrition can supplement stored energy reserves to support developmental processes, and thus could increase the longevity of lipid stores and potential pelagic duration of coral larvae.

iii. Late development: integration of symbiotic metabolism to meet energetic demand

In late development (metamorphosed polyps and attached recruits; 183-255 hpf), host-symbiont metabolic interaction continued to increase, demonstrating a greater contribution of symbiont-derived nutrition to support the energetic demands of metamorphosis and settlement. As observed in larvae, metabolism of both translocated (i.e., glucose and fatty acids) and stored energy reserves (i.e., complex carbohydrates and lipids) are necessary in late development. First, utilization of carbohydrate photosynthates, specifically glucose and galactose (70, 98) in late developmental stages is indicated by enrichment of glucose, hexose, and monosaccharide metabolism, catabolism, and biosynthesis genes (Fig 3C), monosaccharide and galactose metabolism metabolites (Fig 4CD) and the transport of organic compounds (Fig 3E). Available glucose pools and pyruvate products of glycolysis peak in late developmental stages along with reduced pools of glucose-6-phosphate intermediates, suggesting peak glucose metabolism through the glycolysis pathway as discussed above (Fig 6A). Further, expression of genes involved in carbohydrate and glucose metabolism remain high after reaching a peak in larvae and metamorphosed polyps at 231 hpf ($p<0.001$; Table S1) (Fig 5AB). These results show that continued metabolism of symbiont-derived glucose is a major component of coral metabolism during metamorphosis and settlement. In addition, fatty acid beta-oxidation and metabolism genes (Fig 3D) continued to be expressed corresponding to the enrichment of short chain acids and derivative metabolites (Fig 4C) and genes involved in organic acid transport (Fig 3E). Fatty acid metabolism gene expression peaked during metamorphosis and continued into the attached recruit stage ($p<0.001$; Table S1) (Fig 5F). These results suggest that along with carbohydrates, fatty acids are an important product of symbiont nutritional exchange for coral development.

In addition to symbiotic nutritional exchange, metabolism of stored reserves is required in late development. There was enrichment of lipid metabolism genes including neutral lipid metabolism, lipid oxidation, lipid biosynthesis, and lipid catabolism in these stages, suggesting continued usage of wax ester stores (Fig 3D). Genes involved in lipid metabolism peaked in metamorphosed polyps, providing additional evidence that metabolism of stored reserves is required to undergo the expensive metamorphosis process (28). Notably, the enrichment of

genes involved in triacylglycerides (also referred to as triglycerides), emerged in late development (i.e., triglyceride metabolic process) (Fig 3D). In several studies, triacylglycerols are present and metabolized in symbiotic larvae, but not in aposymbiotic larvae (19, 20, 22), and is therefore an indicator that symbiont-derived lipid products are synthesized into triacylglyceride stores in the host and can be used to meet energy demand. Molecular and metabolomic evidence also revealed that complex storage carbohydrates were metabolized in attached recruits indicated by enrichment of disaccharide metabolites and starch and sucrose metabolic pathways (Fig 4CD) in addition to expression of other storage carbohydrates including glycogen, cellular glycan, and glucan metabolism genes (Fig 3C) (99, 100). Therefore, the capacity to supplement energy demand with symbiotic nutrition can extend the period of lipid catabolism during larval stages, potentially expanding post-settlement survival and recruitment potential in vertical transmitters (22).

Our results demonstrate that the post-settlement energetic demand requires the utilization of translocated and stored sources of carbohydrates in *M. capitata* late developmental stages. This supports previous hypotheses by (23, 101) that nutritional exchange is more meaningful to post-settlement energy demand than in larval stages. This is also consistent with observations that under other energetically stressful conditions, such as thermal stress bleaching, pools of both simple and complex carbohydrates are depleted (99, 102). Additionally, utilization of carbohydrate resources in attached recruit stages may be in response to energy requirements of early calcification (103, 104). Indeed, in late development, there was upregulation of inorganic ion and cation import across plasma membranes (Fig 3E) and bicarbonate transport (Fig 5E), which transports ions to the site of calcification (105). Another indicator that nutritional exchange is occurring in attached recruits is through the enrichment of phenylalanine, tyrosine, and tryptophan metabolism (Fig 4D), which are essential amino acids translocated from the symbiont (106) and facilitated by amino acid transmembrane transport genes (Fig 4E) (81).

As observed in larvae, corals employ cellular stress management mechanisms to maintain a stable symbiotic relationship. As discussed above, ammonium metabolism and nitrogen homeostasis functions are continued, indicated by increased expression of ammonium metabolism genes (Fig 5G) and a peak in glutamine pools (Fig 6C), suggesting high glutamine synthase pathway activity. Further, ROS regulation, sphingolipid and ceramide metabolism, and sterol transport genes were expressed in late development (Fig 3E), which have been shown to assist with mitigating cellular stress and increasing membrane stability (95, 97). Production of methionine sulfoxide antioxidant metabolites peaks in attached recruits ($p<0.001$; Table S1) (Fig 6D) and gene expression of oxidative stress genes peaks in metamorphosed polyps ($p<0.001$; Table S1) (Fig 6H). ROS damage and transcriptional responses have also been seen in symbiotic *Acropora intermedia* larvae (144-216 hpf) under increased temperatures (96), corresponding to the stages where we observed enrichment in ROS regulation in mid and late developmental stages (65 hpf through 231 hpf). In addition to redox balance challenges and free radical repair, increases in energetic stress during metamorphosis and recruitment may enable pathogenic infections (107). We documented enrichment in anti-microbial metabolic pathways (i.e., neomycin, kanamycin, gentamicin biosynthesis) (44, 108, 109) in recruits (Fig 4D), which may result from defense to pathogenic infections and/or defense against benthic microbial communities during settlement (110). These results demonstrate that metabolic

interaction and integration between the host and Symbiodiniaceae increases in late development, representing an ontogenetic window that relies heavily on the input of symbiotic nutrition in vertically transmitting species to progress through the costly process of metamorphosis and settlement. Further, this integration of the symbiotic relationship requires cellular mechanisms of management and investment to maintain a stable and productive nutritional exchange.

D. Conclusions

In this study, we show that nutritional exchange between Symbiodiniaceae and corals is important to meet energetic demands of development and buffer the requirements for energetic reserves. As climate change stressors increase, successful reproduction and recruitment is critical for coral reefs to persist (18, 35, 111). Because development is energetically demanding (15), access to symbiont-derived resources may buffer these costs for vertically transmitting species. Critically, our integrative approach across a developmental time series in *M. capitata* revealed that in larval stages, symbiont-host nutritional exchange begins, followed by increased utilization of photosynthetic products through metamorphosis and settlement (Fig 7). Increased metabolic interaction in attached recruits shows that symbiotic nutrition is an important energy source in addition to stored reserves as early life stages progress through settlement (Fig 7). Therefore, heatwave conditions that stress the symbiotic relationship could damage or delay the onset of nutritional exchange and may exacerbate energetic vulnerabilities during recruitment.

We demonstrate that the energetic costs of development and demands against the limited bank of energy reserves can be buffered by symbiont-derived nutrition in vertically transmitting corals, especially in post-settlement stages and could outweigh energetic vulnerabilities to symbiotic environmental stress (24). However, in horizontal transmission species, the dominant reproductive strategy in reef-building corals (16), the metabolic contribution of symbiont-derived nutrition will depend on the timing of symbiont acquisition and can vary across larval to recruit stages (101). As developmental costs increase with climate change (15), access to symbiotic nutrition earlier in development may provide energetic advantages to horizontal transmitters. Most critically, reducing environmental stress and bleaching conditions during the larval and post-metamorphosis stages when nutritional exchange is being established and is essential to meet energy requirements could be a key intervention to enhance recruitment and post-settlement survival on reefs.

Materials and Methods

All raw and processed data and bioinformatic and statistical code are archived openly and are available at https://github.com/AHuffmyer/EarlyLifeHistory_Energetics/releases/tag/v2.0.0 and Open Science Framework (112). Raw sequence files are stored on the NCBI Sequence Read Archive under project PRJNA900235.

A. Gamete collection and developmental rearing

Montipora capitata is a hermaphroditic broadcast spawning, vertically transmitting coral species that is a dominant reef-builder in Kāne□ohe Bay, O□ahu, Hawai□i where this study was conducted (Fig 1B). During the July 2020 spawning period, *M. capitata* egg and sperm bundles were collected on the night of the new moon (21:00 h) by scooping spawned bundles from the surface of the water in Kāne□ohe Bay. Bundles were then transported to the laboratory at the Hawai□i Institute of Marine Biology (HIMB), fertilized at 27.5°C and added to 20 L conical rearing vessels (*N* =30) supplied with 1 µm filtered seawater (FSW) at 27.5°C and <50 µmol photons m^{-2} s^{-1} (photosynthetic active radiation; PAR) (Fig 1B). Embryos were reared in conical vessels through development to the swimming larval stage (Fig 1B). At approximately 165 hours post-fertilization, larvae were transferred in 53 µm mesh-bottom plastic bins to outdoor flow-through seawater tables for settlement containing aragonite settlement plugs (circular surface; surface area 2.85 cm^2) conditioned for 3 days in seawater. Settlement was conducted at ambient temperature (~28°C) and light of <100 µmol m^{-2} s^{-1} PAR. Two settlement states were sampled in this study - larvae that metamorphosed and attached to the surface of aragonite plugs (Fig 1B) and those that metamorphosed without attachment (i.e., metamorphosed polyps). We sampled time points across the early life history of *M. capitata* including fertilized eggs (1-hour post-fertilization, hpf), embryos (cleavage at 5 hpf, late gastrula stage at 38 and 65 hpf), larvae (93, 163, 183, 231 hpf), metamorphosed polyps (83 and 213 hpf), and attached recruits (183, 231, and 255 hpf) (Fig 1A) for molecular, metabolomic, physiological, and amplicon sequencing assays. Detailed methods for this study are described in Supplementary Materials.

B. Respirometry

Respiration (oxygen consumption) and photosynthesis (oxygen production) rates were measured using an Oxy-10 Sensor Dish Reader (PreSens Precision Sensing) in combination with a 24-well microplate with spot oxygen sensors (80 µL; Loligo Systems) at six time points: embryos (65 hpf), larvae (93, 183, and 231 hpf) and metamorphosed polyps (183 and 231 hpf) (Fig 1A). Six individuals were added to each microplate well filled with 1 µm FSW and sealed with glass coverslips. Oxygen production (photosynthesis) was first measured under light conditions (~500 PAR) followed by measurement of light-enhanced dark respiration (LEDR, hereafter referred to as “respiration”). All measurements were conducted at 28°C. Light levels during photosynthesis measurements are within the saturating irradiance for adults of this species (113), but PI curves were not conducted at the early life stages and therefore, we only focus on relative comparisons between life stages in this study. Photosynthesis and respiration rates were extracted using localized linear regressions and calculated as nmol O_2 $individual^{-1}$ min^{-1}. Photosynthesis:respiration ratios (P:R) were calculated as gross photosynthesis divided by respiration. Normality of residual and homogeneity of variance were assessed using quantile-quantile plots and Levene’s tests in the *car* package, respectively (114) R Statistical Programming v4.2.2 (115). Posthoc comparisons were conducted using a Tukey p-value adjustment in the *emmeans* package (116).

C. Size and symbiont cell density

At each time point (Fig 1A), individuals were collected across multiple rearing vessels (*n* = 3-5 conicals or bins), pooled, fixed in 4% paraformaldehyde for 24-36 h then stored in 70% ethanol at 4°C (*n* = 4 samples per time point; approx. 100 individuals per sample) for size and symbiont density measurements. Samples were digitally photographed using a dissecting light microscope with a stage micrometer. Size was calculated as the volume of randomly selected individuals (*n* = 15) from each sample in ImageJ (117) using equations that approximate the volume for each life stage (Supplementary Materials). We did not measure the size of attached recruits on plugs because recruits often settled in aggregation, preventing measurement of individual size. We tested for differences in size between life stage time points using a non-parametric Kruskal Wallis test.

Symbiont cell density at each developmental time point (Fig 1A) was measured by conducting replicate cell counts (n = 6-8) of homogenized tissue using a hemocytometer and normalizing to the number of individuals in the sample (egg through metamorphosed polyps; cells individual^{-1}), or total surface area of tissue sampled (attached recruits; cells mm^{-2}). Symbiont densities were analyzed using a one-way ANOVA test with developmental time point as the main effect. Differences in symbiont cell densities between time points in attached recruits (symbiont cells per mm^{2}) were analyzed separately using a non-parametric Kruskal Wallis test.

D. Gene expression in the coral host

Samples were preserved in DNA/RNA Shield (Zymo Research) or obtained from tissue scraped from settlement plugs that were snap-frozen in liquid nitrogen (Fig 1A). RNA and DNA extractions were performed with the Quick DNA/RNA Miniprep Plus Kit (Zymo Research Catalog #D7003) according to the manufacturer's instructions (see protocol in data repository; (112)). We sequenced RNA using TagSeq, which is a 3' short transcript method that is a cost-effective alternative to RNAseq and allows for accurate estimates of transcript abundance (59). Library preparation was adapted for sequencing on one lane of Illumina NovaSeq 6000 SR100 with standard coverage of 3-5 million 100 bp single end reads (University of Texas Austin, Genomic Sequencing and Analysis Facility). Sequence reads were trimmed and filtered for quality control and aligned and mapped to the *M. capitata* reference assembly (118) to generate a gene count matrix (see Supplementary Materials and code repository for full details).

Gene expression across developmental time points was first visualized using PCA analyses and tested using a permutational analysis of variance (PERMANOVA) in the *vegan* package (119). Gene expression was then analyzed using a weighted gene co-expression network analysis (WGCNA) in the *WGCNA* package (61) and assigned to modules by expression pattern. Functional enrichment of genes in each module was conducted by analyzing the list of genes associated with each ontogenetic pattern using gene ontology (GO) enrichment analysis in GOSeq (120) and published functional annotation accompanying the reference genome (118). Significantly enriched GO terms were filtered to select terms of interest related to carbohydrate metabolism, lipid metabolism, and communication and transport and expression of genes involved in key pathways were analyzed separately across development using one-way ANOVAs (Supplementary Materials). We further examined expression of genes involved in specific pathways by selecting genes with GO terms with terms of interest.

E. Metabolomics

Samples for metabolomic analysis were snap-frozen in liquid nitrogen and stored at -80°C (Fig 1A). Metabolites were extracted from the coral host fraction using 40:40:20 methanol:acetonitrile:water with 0.5%[v/v] formic acid according to (60) and identified and quantified at the Rutgers Cancer Institute of New Jersey Metabolomics facility using hydrophilic interaction liquid chromatography separation and liquid chromatography-mass spectrometry (LC-MS) quantification (Supplementary Materials). Ion counts for identified metabolites were center normalized to the respective sample median and $\log_{10}$ transformed. We examined metabolomic profiles across development using supervised partial least squares discriminant analysis (PLS-DA) in the *mixOmics* package (121). To detect metabolites that correlated with developmental time points, we conducted a weighted correlation network analysis (WCNA) in the *WGCNA* package (61) Metabolites were then analyzed for enrichment of compound class and KEGG pathways using the list of metabolites associated with each ontogenetic pattern in MetaboAnalyst 5.0 web interface (122). Metabolites involved in key pathways of interest were also examined separately using one-way ANOVAs, including metabolites involved in glycolysis, ammonium metabolism, energy carrier metabolism, and antioxidant metabolites (Supplementary Materials).

F. ITS2 amplicon sequencing

ITS2 amplicon sequencing was conducted to identify Symbiodiniaceae communities from extracted DNA across time points (Fig 1A). A two-step PCR protocol was used to prepare PCR products for sequencing according to a modification of the Illumina 16S Metagenomic Sequencing Library Preparation protocol (see protocol in data repository; (112)) to amplify the ITS2 region of Symbiodiniaceae nuclear ribosomal DNA using published primers (123). Samples were sequenced on an Illumina MiSeq platform (Illumina, San Diego, CA) using 2x300 bp paired-end sequencing at the RI-INBRE Molecular Informatics Core (Kingston, RI). Sequences were quality controlled and subsampled to even sequencing depth and analyzed locally to identify Symbiodiniaceae Defining Intragenomic Variants (DIVs) that determine ITS2 type profiles using the SymPortal workflow (124). Relative abundance was calculated and visualized for DIVs at >1% relative abundance. Alpha diversity of DIVs was calculated using Shannon and Inverse Simpson indices and analyzed using one-way ANOVA with time point as the main effect. Shifts in Symbiodiniaceae communities (Bray-Curtis dissimilarity) were visualized across ontogeny using a non-metric multidimensional scaling analysis (NMDS) in the *phyloseq* package (125).

G. 16S rRNA amplicon sequencing

To identify microbial communities, we conducted 16S rRNA amplicon sequencing across development (Fig 1A). Extracted DNA was prepared using a two-step PCR protocol using published primers for the 16S rRNA V4 variable region (126). Samples were then sequenced on an Illumina MiSeq (Illumina, San Diego, CA) for 2x300 bp paired-end sequencing at the RI-

INBRE Molecular Informatics Core. We conducted data analysis using the *mothur* analytical pipeline (v1.46.1) (127) including filtering, alignment to the Silva database (release 138.1; (128)), removal of chimeras, and subsampling (900 sequences) to quantify operational taxonomic units (OTU). Due to low bacterial sequences, 13 out of 39 samples were removed after subsampling. The removed samples included egg (1 hpf), embryo (5 hpf), and half of the samples at 38 and 65 hpf stages, indicating low bacterial sequences generated from the earliest life stages in the time series, which corresponded to samples with low DNA concentration during extraction. These samples were not included in further analysis.

OTU count tables were then analyzed in R using the *phyloseq* package (125). Shifts in bacterial communities (Bray-Curtis dissimilarity) across ontogeny were visualized using a non-metric multidimensional scaling analysis (NMDS). Taxa abundance was calculated as percent relative abundance and filtered to those present at >0.5% for visualization at the genus level. Alpha diversity was calculated using Shannon and Inverse Simpson indices. Changes in alpha diversity across development were analyzed using a one-way ANOVA with time point as the main effect.

Funding

This research was supported by the National Science Foundation Ocean Sciences Postdoctoral Fellowship to ASH (award no. 2205966), US-Israeli Binational Science Foundation to HMP and TM (award no. BSF 2016-321), National Science Foundation Rules of Life-Epigenetics (award no. EF-1921465) and was supported by a gift of the Washington Research Foundation to the University of Washington eScience Institute.

Acknowledgements

We are grateful for the logistical support provided by the Coral Resilience Lab and the Hawai□i Institute of Marine Biology. We acknowledge Margaret Schedl for RNA extraction, Craig Nelson and Shayle Matsuda for discussions on 16S bacterial analyses, David Beck for assistance with integrative analysis and computing, Eric Chiles and Xiaoyang Su for metabolomics discussions, and the Putnam (University of Rhode Island) and Roberts Labs (University of Washington) for feedback on earlier versions of this manuscript. We acknowledge use of the computational resources of the URI Center for Computational Research for this work. As guests, we recognize and give thanks for the land and water resources of the ’āina and the traditional owners of the land, kānaka ’ōiwi, both past and present, as well as future generations, on which this experimental work was conducted in the Kāne□ohe Ahupua’a and the islands of Hawai’i.

Data Availability

Data and scripts are available on GitHub at https://github.com/AHuffmyer/EarlyLifeHistory_Energetics/releases/tag/v2.0.0 and Open Science Framework (OSF) (112). Raw sequence files (TagSeq, ITS2, and 16S) are stored at

the NCBI Sequence Read Archive under project PRJNA900235. Raw and processed metabolomic data are archived at OSF (112).

Author Contributions

Author contributions: A.S.H. and H.M.P. designed research; A.S.H. performed research and sample collection; A.S.H., K.H.W., D.M.B., and E.S. collected and analyzed data; A.S.H. wrote the manuscript and K.H.W, D.M.B., E.S., T.M., and H.M.P. revised the manuscript. All authors approved the final submission.

References

1. L. Muscatine, J. W. Porter, Reef Corals: Mutualistic Symbioses Adapted to Nutrient-Poor Environments. *Bioscience* **27**, 454–460 (1977).

2. T. C. LaJeunesse, *et al.*, Systematic revision of Symbiodiniaceae highlights the antiquity and diversity of coral endosymbionts. *Curr. Biol.* **28**, 2570–2580 (2018).

3. L. Muscatine, L. R. Mccloskey, R. E. Marian, Estimating the daily contribution of carbon from zooxanthellae to coral animal respiration. *Limnol. Oceanogr.* **26**, 601–611 (1981).

4. P. G. Falkowski, Z. Dubinsky, L. Muscatine, J. W. Porter, Light and the bioenergetics of a symbiotic coral. *Bioscience* **34**, 705–709 (2006).

5. P. G. Falkowski, Z. Dubinsky, L. Muscatine, L. McCloskey, Population control in symbiotic corals - Ammonium ions and organic materials maintain the density of zooxanthellae. *Bioscience* **43**, 606–611 (1993).

6. S. Roberty, E. Béraud, R. Grover, C. Ferrier-Pagès, Coral Productivity Is Co-Limited by Bicarbonate and Ammonium Availability. *Microorganisms* **8** (2020).

7. D. G. Bourne, K. M. Morrow, N. S. Webster, Insights into the Coral Microbiome: Underpinning the Health and Resilience of Reef Ecosystems. *Annu. Rev. Microbiol.* **70**, 317–340 (2016).

8. S. R. Connolly, D. R. Bellwood, T. P. Hughes, Indo-pacific biodiversity of coral reefs: Deviations from a mid-domain model. *Ecology* **84**, 2178–2190 (2003).

9. A. J. Woodhead, C. C. Hicks, A. V. Norström, G. J. Williams, N. A. J. Graham, Coral reef ecosystem services in the Anthropocene. *Funct. Ecol.* **33**, 1023-1034 (2019).

10. V. M. Weis, Cellular mechanisms of Cnidarian bleaching: stress causes the collapse of symbiosis. *J. Exp. Biol.* **211**, 3059–3066 (2008).

11. S. Sully, D. E. Burkepile, M. K. Donovan, G. Hodgson, R. van Woesik, A global analysis of coral bleaching over the past two decades. *Nat. Commun.* **10**, 1264 (2019).

12. T. D. Eddy, *et al.*, Global decline in capacity of coral reefs to provide ecosystem services. *One Earth* **4**, 1278–1285 (2021).

13. R. Ritson-Williams, *et al.*, New perspectives on ecological mechanisms affecting coral recruitment on reefs. *Smithson. Contrib. Mar. Sci.* **38**, 437–457 (2009).

14. J. Pineda, Linking larval settlement to larval transport: assumptions, potentials, and pitfalls. *Oceanography of the eastern Pacific* **1**, 84–105 (2000).

15. D. J. Marshall, A. K. Pettersen, M. Bode, C. R. White, Developmental cost theory predicts thermal environment and vulnerability to global warming. *Nature Ecology and Evolution* **4**, 406–411 (2020).

16. A. H. Baird, J. R. Guest, B. L. Willis, Systematic and Biogeographical Patterns in the Reproductive Biology of Scleractinian Corals. *Annu. Rev. Ecol. Evol. Syst.* **40**, 551–571 (2009).

17. S. L. Rosset, *et al.*, The Molecular Language of the Cnidarian–Dinoflagellate Symbiosis. *Trends Microbiol.* **29**, 320-333 (2020).

18. P. J. Edmunds, Coral recruitment: patterns and processes determining the dynamics of coral populations. *Biol. Rev. Camb. Philos. Soc.* (2023) https:/doi.org/10.1111/brv.12987.

19. S. Harii, K. Nadaoka, M. Yamamoto, K. Iwao, Temporal changes in settlement, lipid content and lipid composition of larvae of the spawning hermatypic coral *Acropora tenui*s. *Mar. Ecol. Prog. Ser.* **346**, 89–96 (2007).

20. J. Figueiredo, *et al.*, Ontogenetic change in the lipid and fatty acid composition of scleractinian coral larvae. *Coral Reefs* **31**, 613–619 (2012).

21. M. R. Gaither, R. Rowan, Zooxanthellar symbiosis in planula larvae of the coral *Pocillopora damicornis*. *J. Exp. Mar. Bio. Ecol.* **386**, 45–53 (2010).

22. S. Harii, M. Yamamoto, O. Hoegh-Guldberg, The relative contribution of dinoflagellate photosynthesis and stored lipids to the survivorship of symbiotic larvae of the reef-building corals. *Mar. Biol.* **157**, 1215–1224 (2010).

23. C. Kopp, I. Domart-Coulon, D. Barthelemy, A. Meibom, Nutritional input from dinoflagellate symbionts in reef-building corals is minimal during planula larval life stage. *Sci Adv* **2**, e1500681 (2016).

24. B. Nesa, A. H. Baird, S. Harii, I. Yakovleva, M. Hidaka, Algal symbionts increase DNA damage in coral planulae exposed to sunlight. *Zool. Stud.* **51**, 6 (2012).

25. B. Mos, S. A. Dworjanyn, Early metamorphosis is costly and avoided by young, but physiologically competent, marine larvae. *Mar. Ecol. Prog. Ser.* **559**, 117–129 (2016).

26. J. A. Pechenik, Larval experience and latent effects--metamorphosis is not a new beginning. *Integr. Comp. Biol.* **46**, 323–333 (2006).

27. N. Okubo, H. H. Yamamoto, F. Nakaya, K. Okaji, Oxygen consumption of a single embryo/planula in the reef-building coral *Acropora intermedia*. *Mar. Ecol. Prog. Ser.* **366**, 305–309 (2008).

28. P. J. Edmunds, V. R. Cumbo, T.-Y. Fan, Metabolic costs of larval settlement and metamorphosis in the coral *Seriatopora caliendrum* under ambient and elevated pCO2. *J.*

Exp. Mar. Bio. Ecol. **443**, 33–38 (2013).

29. L. C. Grasso, *et al.*, The biology of coral metamorphosis: molecular responses of larvae to inducers of settlement and metamorphosis. *Dev. Biol.* **353**, 411–419 (2011).

30. S. Tambutté, *et al.*, Coral biomineralization: From the gene to the environment. *J. Exp. Mar. Bio. Ecol.* **408**, 58–78 (2011).

31. M. Gilis, *et al.*, Biomineralization in newly settled recruits of the scleractinian coral *Pocillopora damicornis*. *J. Morphol.* **275**, 1349–1365 (2014).

32. L. Allen-Waller, K. L. Barott, Symbiotic dinoflagellates divert energy away from mutualism during coral bleaching recovery. *Symbiosis* **89**, 173-186 (2023).

33. C. J. Randall, A. M. Szmant, Elevated temperature reduces survivorship and settlement of the larvae of the Caribbean scleractinian coral, *Favia fragum* (Esper). *Coral Reefs* **28**, 537–545 (2009).

34. M. Nakamura, S. Ohki, A. Suzuki, K. Sakai, Coral larvae under ocean acidification: survival, metabolism, and metamorphosis. *PLoS One* **6**, e14521 (2011).

35. T. P. Hughes, *et al.*, Global warming impairs stock–recruitment dynamics of corals. *Nature* **568**, 387–390 (2019).

36. C. B. Wall, M. Kaluhiokalani, B. N. Popp, M. J. Donahue, R. D. Gates, Divergent symbiont communities determine the physiology and nutrition of a reef coral across a light-availability gradient. *ISME J.* **14**, 945–958 (2020).

37. M. Helmkampf, M. R. Bellinger, M. Frazier, M. Takabayashi, Symbiont type and environmental factors affect transcriptome-wide gene expression in the coral *Montipora capitata*. *Ecol. Evol.* **9**, 378–392 (2019).

38. R. Cunning, R. Ritson-Williams, R. D. Gates, Patterns of bleaching and recovery of *Montipora capitata* in Kane'ohe Bay, Hawai'i, USA. *Mar. Ecol. Prog. Ser.* **551**, 131–139 (2016).

39. T. C. LaJeunesse, D. J. Thornhill, Improved resolution of reef-coral endosymbiont (*Symbiodinium*) species diversity, ecology, and evolution through psbA non-coding region genotyping. *PLoS One* **6**, e29013 (2011).

40. D. C. Wham, G. Ning, T. C. LaJeunesse, *Symbiodinium glynnii* sp. nov., a species of stress-tolerant symbiotic dinoflagellates from pocilloporid and montiporid corals in the Pacific Ocean. *Phycologia* **56**, 396–409 (2017).

41. T. N. F. Roach, *et al.*, Metabolomic signatures of coral bleaching history. *Nat. Ecol. Evol.* **5**, 495-503 (2020).

42. J. Dilworth, C. Caruso, V. A. Kahkejian, A. C. Baker, C. Drury, Host genotype and stable differences in algal symbiont communities explain patterns of thermal stress response of *Montipora capitata* following thermal pre-exposure and across multiple bleaching events. *Coral Reefs* **40**, 151–163 (2021).

43. J. L. Padilla-Gamiño, X. Pochon, C. Bird, G. T. Concepcion, R. D. Gates, From parent to

gamete: vertical transmission of *Symbiodinium* (Dinophyceae) ITS2 sequence assemblages in the reef building coral *Montipora capitata*. *PLoS One* **7**, e38440 (2012).

44. K. H. Sharp, K. B. Ritchie, Multi-partner interactions in corals in the face of climate change. *Biol. Bull.* **223**, 66–77 (2012).

45. J. L. Matthews, *et al.*, Symbiodiniaceae-bacteria interactions: rethinking metabolite exchange in reef-building corals as multi-partner metabolic networks. *Environ. Microbiol.* **22**, 1675–1687 (2020).

46. T. D. Glaze, D. V. Erler, H. M. P. Siljanen, Microbially facilitated nitrogen cycling in tropical corals. *ISME J.* **16**, 68–77 (2022).

47. N. Radecker, C. Pogoreutz, C. R. Voolstra, J. Wiedenmann, C. Wild, Nitrogen cycling in corals: The key to understanding holobiont functioning? *Trends Microbiol.* **23**, 490–497 (2015).

48. R. S. Peixoto, P. M. Rosado, D. C. de A. Leite, A. S. Rosado, D. G. Bourne, Beneficial Microorganisms for Corals (BMC): Proposed Mechanisms for Coral Health and Resilience. *Front. Microbiol.* **8**, 341 (2017).

49. H. G. Reich, E. F. Camp, L. M. Roger, H. M. Putnam, The trace metal economy of the coral holobiont: supplies, demands and exchanges. *Biol. Rev. Camb. Philos. Soc.* **98**, 623-642 (2022).

50. J. Ceh, *et al.*, Nutrient cycling in early coral life stages: *Pocillopora damicornis* larvae provide their algal symbiont (*Symbiodinium*) with nitrogen acquired from bacterial associates. *Ecol. Evol.* **3**, 2393–2400 (2013).

51. M. J. A. Vermeij, J. E. Smith, C. M. Smith, R. Vega Thurber, S. A. Sandin, Survival and settlement success of coral planulae: independent and synergistic effects of macroalgae and microbes. *Oecologia* **159**, 325–336 (2009).

52. A. D. Williams, B. E. Brown, L. Putchim, M. J. Sweet, Age-Related Shifts in Bacterial Diversity in a Reef Coral. *PLoS One* **10**, e0144902 (2015).

53. N. E. Kimes, J. D. Van Nostrand, E. Weil, J. Zhou, P. J. Morris, Microbial functional structure of *Montastraea faveolata*, an important Caribbean reef-building coral, differs between healthy and yellow-band diseased colonies. *Environ. Microbiol.* **12**, 541–556 (2010).

54. J.-B. Raina, E. A. Dinsdale, B. L. Willis, D. G. Bourne, Do the organic sulfur compounds DMSP and DMS drive coral microbial associations? *Trends Microbiol.* **18**, 101–108 (2010).

55. J.-B. Raina, *et al.*, Isolation of an antimicrobial compound produced by bacteria associated with reef-building corals. *PeerJ* **4**, e2275 (2016).

56. A. Cárdenas, *et al.*, Greater functional diversity and redundancy of coral endolithic microbiomes align with lower coral bleaching susceptibility. *ISME J.* **16**, 2406–2420 (2022).

57. E. M. Sogin, H. M. Putnam, C. E. Nelson, P. Anderson, R. D. Gates, Correspondence of coral holobiont metabolome with symbiotic bacteria, archaea and *Symbiodinium* communities. *Environ. Microbiol. Rep.* **9**, 310–315 (2017).

58. J. P. Engelberts, S. J. Robbins, K. Damjanovic, N. S. Webster, Integrating novel tools to elucidate the metabolic basis of microbial symbiosis in reef holobionts. *Mar. Biol.* **168**, 175 (2021).

59. B. K. Lohman, J. N. Weber, D. I. Bolnick, Evaluation of TagSeq, a reliable low-cost alternative for RNAseq. *Mol. Ecol. Resour.* **16**, 1315–1321 (2016).

60. A. Williams, *et al.*, Metabolomic shifts associated with heat stress in coral holobionts. *Sci Adv* **7**, eabd4210 (2021).

61. P. Langfelder, S. Horvath, WGCNA: an R package for weighted correlation network analysis. *BMC Bioinformatics* **9**, 559 (2008).

62. E. Chille, *et al.*, Developmental series of gene expression clarifies maternal mRNA provisioning and maternal-to-zygotic transition in a reef-building coral. *BMC Genomics* **22**, 815 (2021).

63. N. Okubo, *et al.*, Comparative embryology of eleven species of stony corals (Scleractinia). *PLoS One* **8**, e84115 (2013).

64. A. Reyes-Bermudez, A. Villar-Briones, C. Ramirez-Portilla, M. Hidaka, A. S. Mikheyev, Developmental Progression in the Coral *Acropora digitifera* Is Controlled by Differential Expression of Distinct Regulatory Gene Networks. *Genome Biol. Evol.* **8**, 851–870 (2016).

65. Q. M. Heather, Q. M. Mark, Embryonic development in two species of scleractinian coral embryos: *Symbiodinium* localization and mode of gastrulation. *Evol. Dev.* **9**, 355–367 (2007).

66. Y. H. Fadlallah, Coral Reefs Sexual Reproduction, Development and Larval Biology in Scleractinian Corals: A Review. *Coral Reefs* **2**, 129–150 (1983).

67. S. Ghosh, A. Körte, G. Serafini, V. Yadav, J. Rodenfels, Developmental energetics: Energy expenditure, budgets and metabolism during animal embryogenesis. *Semin. Cell Dev. Biol.* **138**, 83-93 (2022).

68. L. J. Rodrigues, J. L. Padilla-Gamiño, Trophic provisioning and parental trade-offs lead to successful reproductive performance in corals after a bleaching event. *Sci. Rep.* **12**, 18702 (2022).

69. B. R. Gordon, W. Leggat, Symbiodinium—Invertebrate Symbioses and the Role of Metabolomics. *Marine Drugs* **8**, 2546–2568 (2010).

70. M. S. Burriesci, T. K. Raab, J. R. Pringle, Evidence that glucose is the major transferred metabolite in dinoflagellate-cnidarian symbiosis. *J. Exp. Biol.* **215**, 3467–3477 (2012).

71. S. Amjad, *et al.*, Role of NAD+ in regulating cellular and metabolic signaling pathways. *Mol Metab* **49**, 101195 (2021).

72. P. May-Panloup, M. Boguenet, H. E. Hachem, P.-E. Bouet, P. Reynier, Embryo and Its Mitochondria. *Antioxidants (Basel)* **10**, 139 (2021).

73. M. E. Strader, G. V. Aglyamova, M. V. Matz, Molecular characterization of larval development from fertilization to metamorphosis in a reef-building coral. *BMC Genomics*

19, 17 (2018).

74. S. E. Leinbach, K. E. Speare, A. M. Rossin, D. M. Holstein, M. E. Strader, Energetic and reproductive costs of coral recovery in divergent bleaching responses. *Sci. Rep.* **11**, 23546 (2021).

75. S. K. Davy, D. Allemand, V. M. Weis, Cell biology of cnidarian-dinoflagellate symbiosis. *Microbiol. Mol. Biol. Rev.* **76**, 229–261 (2012).

76. J. L. Matthews, *et al.*, Partner switching and metabolic flux in a model cnidarian-dinoflagellate symbiosis. *Proc. Biol. Sci.* **285** (2018).

77. D. Yellowlees, T. A. V. Rees, W. Leggat, Metabolic interactions between algal symbionts and invertebrate hosts. *Plant Cell Environ.* **31**, 679–694 (2008).

78. A. A. Venn, J. E. Loram, A. E. Douglas, Photosynthetic symbioses in animals. *J. Exp. Bot.* **59**, 1069–1080 (2008).

79. M. A. Teece, B. Estes, E. Gelsleichter, D. Lirman, Heterotrophic and autotrophic assimilation of fatty acids by two scleractinian corals, *Montastraea faveolata* and *Porites astreoides*. *Limnol. Oceanogr.* **56**, 1285–1296 (2011).

80. C. Treignier, I. Tolosa, R. Grover, S. Reynaud, C. Ferrier-Pagés, Carbon isotope composition of fatty acids and sterols in the scleractinian coral *Turbinaria reniformis*: Effect of light and feeding. *Limnol. Oceanogr.* **54**, 1933–1940 (2009).

81. E. M. Lehnert, *et al.*, Extensive differences in gene expression between symbiotic and aposymbiotic cnidarians. *G3* **4**, 277–295 (2014).

82. V. Z. Radice, *et al.*, Evaluating coral trophic strategies using fatty acid composition and indices. *PLoS One* **14**, e0222327 (2019).

83. L. A. Morris, C. R. Voolstra, K. M. Quigley, D. G. Bourne, L. K. Bay, Nutrient Availability and Metabolism Affect the Stability of Coral–Symbiodiniaceae Symbioses. *Trends Microbiol.* **27**, 678–689 (2019).

84. O. Rahav, Z. Dubinsky, Y. Achituv, P. G. Falkowski, D. C. Smith, Ammonium metabolism in the zooxanthellate coral, *Stylophora pistillata*. *Proc. R. Soc. B: Biol. Sci.* **236**, 325–337 (1989).

85. M. Pernice, *et al.*, A single-cell view of ammonium assimilation in coral–dinoflagellate symbiosis. *ISME J.* **6**, 1314–1324 (2012).

86. N. Rädecker, *et al.*, Heat stress destabilizes symbiotic nutrient cycling in corals. *Proc. Natl. Acad. Sci. U. S. A.* **118** (2021).

87. J. M. Roberts, L. M. Fixter, P. S. Davies, Ammonium metabolism in the symbiotic sea anemone *Anemonia viridis*. *Hydrobiologia* **461**, 25–35 (2001).

88. E. N. Chiles, *et al.*, Stable isotope tracing reveals compartmentalized nitrogen assimilation in scleractinian corals. *Frontiers in Marine Science*, 2395.

89. G. Cui, *et al.*, Molecular insights into the Darwin paradox of coral reefs from the sea

anemone *Aiptasia*. *Sci Adv* **9**, eadf7108 (2023).

90. M.-F. Lin, S. Takahashi, S. Forêt, S. K. Davy, D. J. Miller, Transcriptomic analyses highlight the likely metabolic consequences of colonization of a cnidarian host by native or non-native *Symbiodinium* species. *Biol. Open* **8**, bio038281 (2019).

91. J. L. Matthews, *et al.*, Optimal nutrient exchange and immune responses operate in partner specificity in the cnidarian-dinoflagellate symbiosis. *Proc. Natl. Acad. Sci. U.S.A.* **114**, 13194–13199 (2017).

92. Y. Su, Z. Zhou, X. Yu, Possible roles of glutamine synthetase in responding to environmental changes in a scleractinian coral. *Mol. Biol. Rep.* **45**, 2115–2124 (2018).

93. A. H. Baird, I. M. Yakovleva, S. Harii, F. Sinniger, M. Hidaka, Environmental constraints on the mode of symbiont transmission in corals. *J. Exp. Mar. Bio. Ecol.* **538**, 151499 (2021).

94. S. A. Kitchen, *et al.*, Coral larvae suppress heat stress response during the onset of symbiosis decreasing their odds of survival. *Mol. Ecol.* **31**, 5813–5830 (2022).

95. S. Levy, *et al.*, A stony coral cell atlas illuminates the molecular and cellular basis of coral symbiosis, calcification, and immunity. *Cell* **184**, 2973–2987 (2021).

96. I. M. Yakovleva, *et al.*, Algal symbionts increase oxidative damage and death in coral larvae at high temperatures. *Marine Ecology Progress Series* **378**, 105–112 (2009).

97. S. A. Kitchen, V. M. Weis, The sphingosine rheostat is involved in the cnidarian heat stress response but not necessarily in bleaching. *J. Exp. Biol.* **220**, 1709–1720 (2017).

98. A. Bertucci, S. Forêt, E. E. Ball, D. J. Miller, Transcriptomic differences between day and night in *Acropora millepora* provide new insights into metabolite exchange and light-enhanced calcification in corals. *Mol. Ecol.* **24**, 4489–4504 (2015).

99. K. E. Hillyer, S. Tumanov, S. Villas-Bôas, S. K. Davy, Metabolite profiling of symbiont and host during thermal stress and bleaching in a model cnidarian-dinoflagellate symbiosis. *J. Exp. Biol.* **219**, 516–527 (2016).

100. C. Kopp, *et al.*, Subcellular investigation of photosynthesis-driven carbon assimilation in the symbiotic reef coral *Pocillopora damicornis*. *MBio* **6**, e02299-14 (2015).

101. M. Mies, P. Y. G. Sumida, N. Rädecker, C. R. Voolstra, Marine Invertebrate Larvae Associated with Symbiodinium: A Mutualism from the Start? *Frontiers in Ecology and Evolution* **5**, 56 (2017).

102. N.-R. Kochman, R. Grover, C. Rottier, C. Ferrier-Pages, M. Fine, The reef building coral *Stylophora pistillata* uses stored carbohydrates to maintain ATP levels under thermal stress. *Coral Reefs* **40**, 1473–1485 (2021).

103. L. Jiang, *et al.*, Diurnally Fluctuating pCO2 Modifies the Physiological Responses of Coral Recruits Under Ocean Acidification. *Front. Physiol.* **9**, 1952 (2018).

104. A. L. Cohen, D. C. Mccorkle, G. A. Gaetani, K. A. Rose, S. de Putron, Morphological and compositional changes in the skeletons of new coral recruits reared in acidified seawater: Insights into the biomineralization response to ocean acidification. *Geochem. Geophys.*

Geosyst. **10**, 1–12 (2009).

105. D. Zoccola, *et al.*, Bicarbonate transporters in corals point towards a key step in the evolution of cnidarian calcification. *Sci. Rep.* **5**, 9983 (2015).

106. J. T. Wang, A. E. Douglas, Essential amino acid synthesis and nitrogen recycling in an alga-invertebrate symbiosis. *Mar. Biol.* **135**, 219–222 (1999).

107. J. M. McDevitt-Irwin, J. K. Baum, M. Garren, R. L. Vega Thurber, Responses of Coral-Associated Bacterial Communities to Local and Global Stressors. *Frontiers in Marine Science* **4**, 262 (2017).

108. S. A. Gignoux-Wolfsohn, S. V. Vollmer, Identification of Candidate Coral Pathogens on White Band Disease-Infected Staghorn Coral. *PLoS One* **10**, e0134416 (2015).

109. D. Meron, *et al.*, Changes in coral microbial communities in response to a natural pH gradient. *ISME J.* **6**, 1775–1785 (2012).

110. H. Jorissen, *et al.*, Coral larval settlement preferences linked to crustose coralline algae with distinct chemical and microbial signatures. *Scientific Reports* **11**, 14610 (2021).

111. T. P. Hughes, J. E. Tanner, Recruitment failure, life histories, and long-term decline of Caribbean corals. *Ecology* **81**, 2250–2263 (2000).

112. A. S. Huffmyer, Cross-scale and multi-omic integration reveals transitions to symbiotic nutritional integration across coral ontogeny (2023) https:/doi.org/10.17605/OSF.IO/KMU7H.

113. E. M. Gibbin, H. M. Putnam, R. D. Gates, M. R. Nitschke, S. K. Davy, Species-specific differences in thermal tolerance may define susceptibility to intracellular acidosis in reef corals. *Mar. Biol.* **162**, 717–723 (2015).

114. J. Fox, S. Weisberg, *An R Companion to Applied Regression*, Second (SAGE Publications, 2018).

115. R Core Team, *R: A language and environment for statistical computing* (R Foundation for Statistical Computing, 2022).

116. R. Lenth, *emmeans: Estimated Marginal Means, aka Least-Squares Means* (2018).

117. C. T. Rueden, *et al.*, ImageJ2: ImageJ for the next generation of scientific image data. *BMC Bioinformatics* **18**, 529 (2017).

118. T. G. Stephens, *et al.*, High-quality genome assemblies from key Hawaiian coral species. *Gigascience* **11** (2022).

119. J. Okansen, et al., *vegan: Community Ecology Package* (2017).

120. M. D. Young, M. J. Wakefield, G. K. Smyth, A. Oshlack, Gene ontology analysis for RNA-seq: accounting for selection bias. *Genome Biol.* **11**, R14 (2010).

121. F. Rohart, B. Gautier, A. Singh, K.-A. Lê Cao, mixOmics: An R package for ’omics feature selection and multiple data integration. *PLoS Comput. Biol.* **13**, e1005752 (2017).

122. Z. Pang, *et al.*, MetaboAnalyst 5.0: narrowing the gap between raw spectra and functional insights. *Nucleic Acids Res.* **49**, W388–W396 (2021).

123. T. C. Lajeunesse, R. K. Trench, Biogeography of two species of *Symbiodinium* (Freudenthal) inhabiting the intertidal sea anemone *Anthopleura elegantissima* (Brandt). *Biol. Bull.* **199**, 126–134 (2000).

124. B. C. C. Hume, *et al.*, SymPortal: A novel analytical framework and platform for coral algal symbiont next-generation sequencing ITS2 profiling. *Mol. Ecol. Resour.* **19**, 1063–1080 (2019).

125. P. J. McMurdie, S. Holmes, phyloseq: an R package for reproducible interactive analysis and graphics of microbiome census data. *PLoS One* **8**, e61217 (2013).

126. A. Apprill, S. McNally, R. Parsons, L. Weber, Minor revision to V4 region SSU rRNA 806R gene primer greatly increases detection of SAR11 bacterioplankton. *Aquat. Microb. Ecol.* **75**, 129–137 (2015).

127. P. D. Schloss, *et al.*, Introducing *mothur*: open-source, platform-independent, community-supported software for describing and comparing microbial communities. *Appl. Environ. Microbiol.* **75**, 7537–7541 (2009).

128. C. Quast, *et al.*, The SILVA ribosomal RNA gene database project: improved data processing and web-based tools. *Nucleic Acids Res.* **41**, D590–6 (2013).

Figures

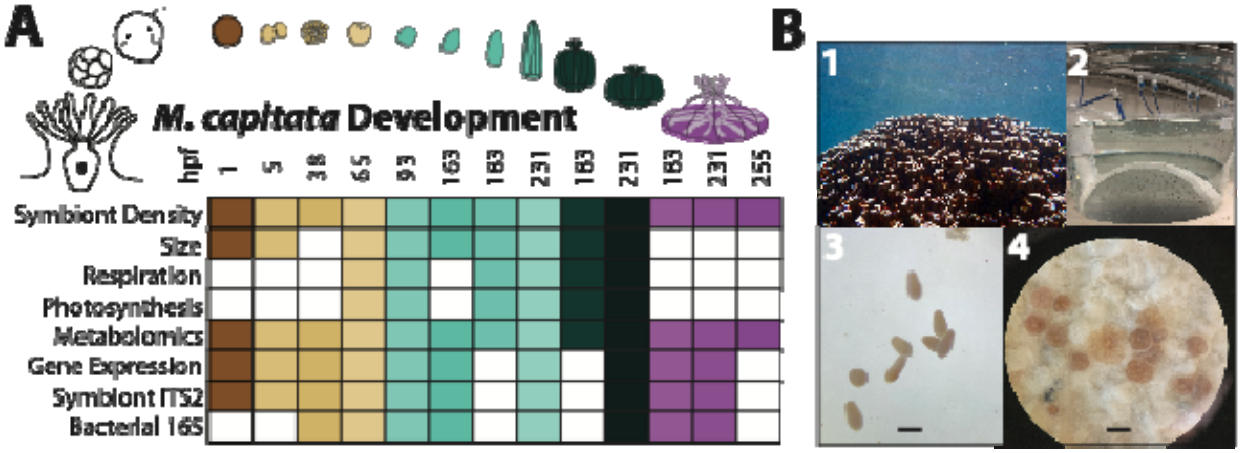

Fig 1. Study overview. (A) Variables measured across *Montipora capitata* development. Filled squares indicate the response variable was sampled at the respective time point; white squares indicate the response was not measured or data is not available. Color corresponds to major life history grouping (eggs=brown, embryos=yellow, larvae=cyan, metamorphosed polyps=green, attached recruits=pink). Hpf indicates hours post fertilization. (B) Photographs of 1 - *M. capitata* colony; 2 - Conical larval rearing chambers; 3 - Planula larvae, note pigmentation due to presence of symbiont cells, scale bar represents 1 mm; 4 - Attached recruits on settlement plug, scale bar represents 1 mm.

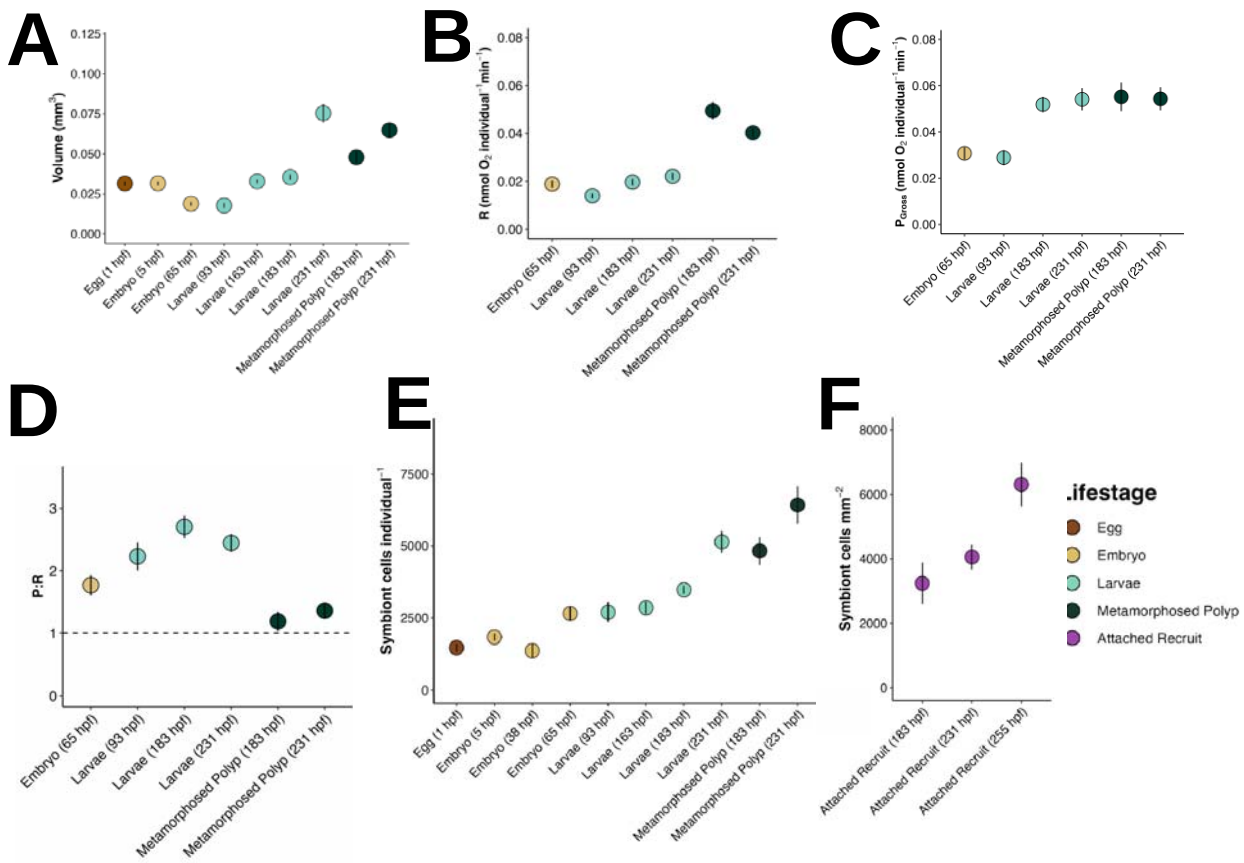

Fig 2. Metabolic rates and physiological responses across *Montipora capitata* development. (A) Size, calculated as volume (mm^3), of each life stage across development. (B) Respiration (oxygen consumed; µmol O_2 individual^{-1} min^{-1}). (C) Gross photosynthesis (oxygen produced; µmol O_2 individual^{-1} min^{-1}). (D) Gross photosynthesis : respiration ration (P:R). Dotted line indicates P:R of 1:1. (E) Symbiont cell density (cells per individual) across development for egg through metamorphosed polyp stages. (F) Symbiont cell density (cells per mm^2) in attached recruits. Data are represented as mean ± standard error for all responses. Developmental time point is indicated on the x-axis with colors indicating life stage. Color corresponds to major life history grouping (eggs=brown, embryos=yellow, larvae=cyan, metamorphosed polyps=green, attached recruits=pink). hpf indicates hours post fertilization.

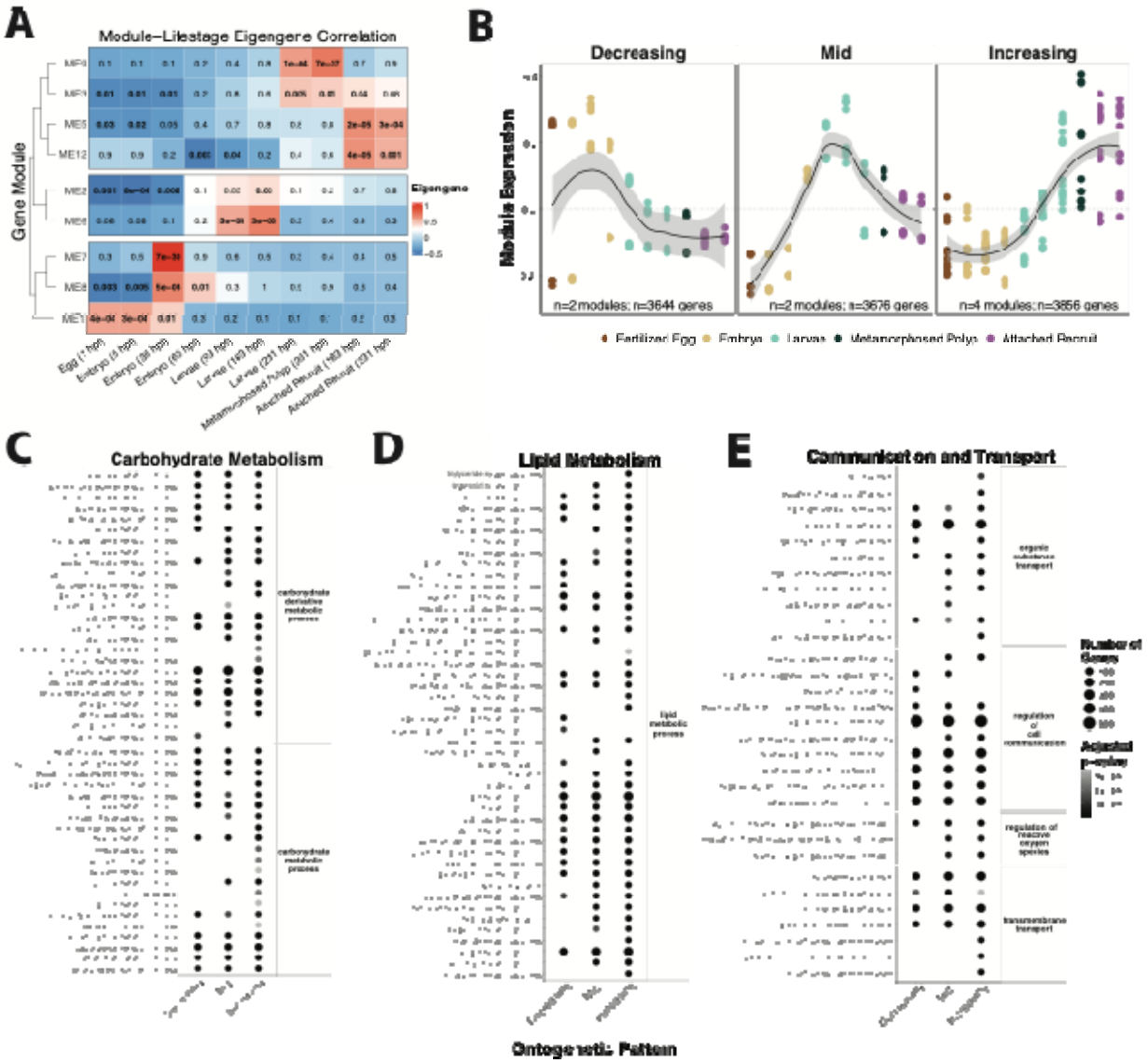

Fig 3. Gene expression across *Montipora capitata* ontogeny. (A) WGCNA analysis with modules of genes (y axis, named as ME#) with positive eigengene expression (red) and negative expression (blue) correlated with lifestage (x axis). Bold values indicate a module is significantly related to the respective lifestage ($p<0.05$). (B) Modules were characterized by the ontogenetic pattern of eigengene expression (y axis) - decreasing across development, peaking in mid-development, or increasing across development. Mean eigengene expression data are shown as dots with life stage groupings indicated by colors (eggs=brown, embryos=yellow, larvae=cyan, metamorphosed polyps=green, attached recruits=pink). Trends lines were plotted using the loess method. Genes in modules of each pattern were functionally annotated using GOSeq at the Biological Process ontology. Significantly enriched GO terms ($p<0.001$) displayed for terms related to (C) carbohydrate metabolism, (D) lipid metabolism, and (E) communication and transport. Size indicates number of genes included in category; color indicates adjusted p-value.

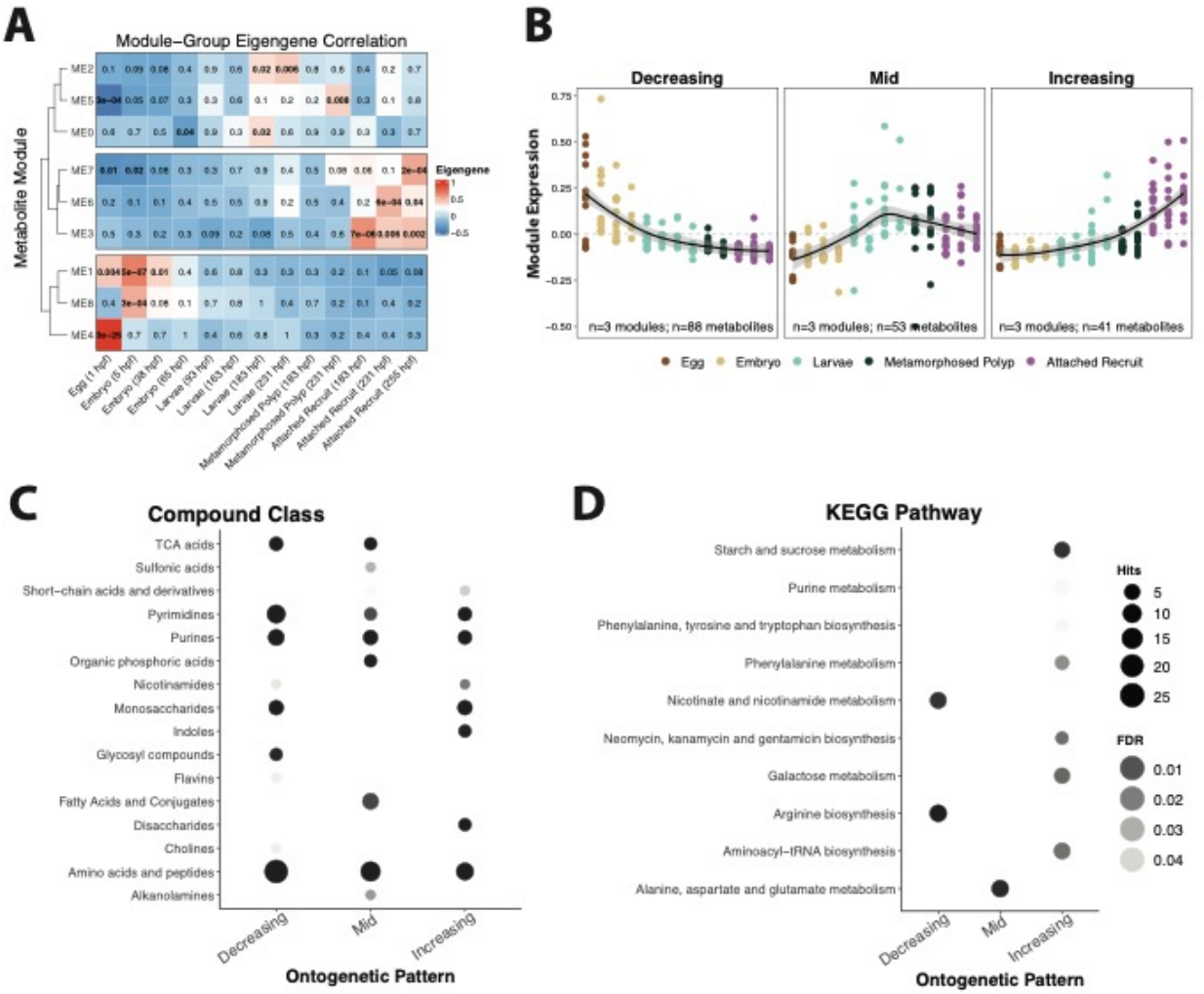

Fig 4. Metabolomics across *Montipora capitata* ontogeny. (A) WCNA analysis with modules of metabolites (y axis) with positive eigengene expression (red) and negative expression (blue) correlated with lifestage (x axis). Bold values indicate a module is significantly related to the respective lifestage ($p<0.05$). (B) Modules were characterized by the ontogenetic pattern of eigengene expression (y axis) - decreasing across development, peaking in mid-development, or increasing across development. Mean module expression values are shown as dots with life stage groupings indicated by colors (eggs=brown, embryos=yellow, larvae=cyan, metamorphosed polyps=green, attached recruits=pink). Trends were plotted using the loess method. Metabolites in modules of each pattern were functionally annotated using MetaboAnalyst for (C) compound classes and (D) KEGG pathways. Size indicates number of metabolites ("Hits") included in category; color indicates adjusted p-value.

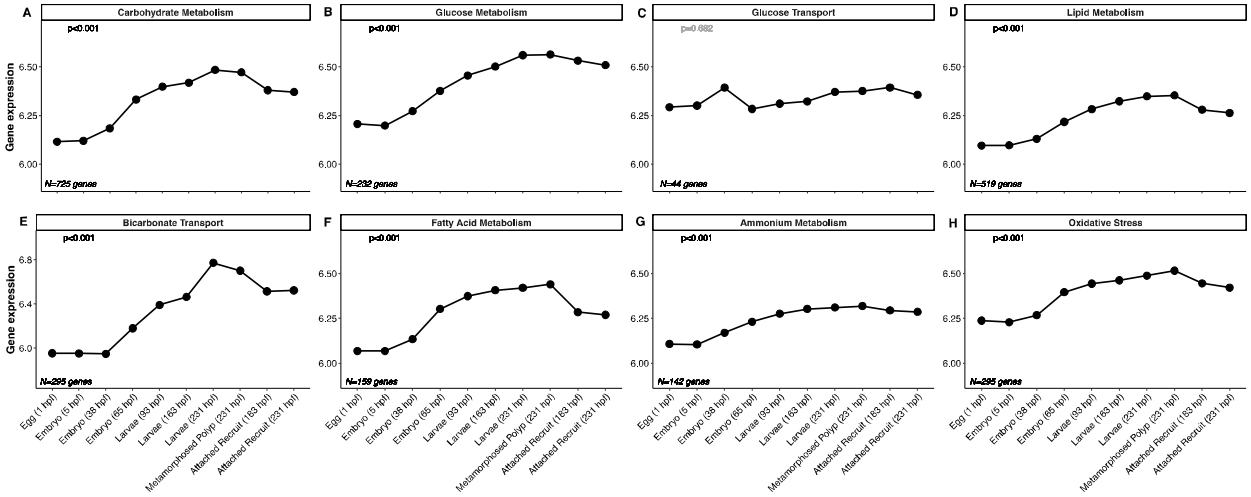

Fig 5. Expression of genes involved in key metabolic pathways across *Montipora capitata* development. Gene expression presented as mean ± standard error of variance stabilized transformed gene counts across life stages. Note that standard error bars are smaller than the points representing the mean and therefore are not visible. N indicates the number of genes included in each category. p-value indicates significance of life stage effects on gene expression (black indicates p<0.05; gray indicates p>0.05).

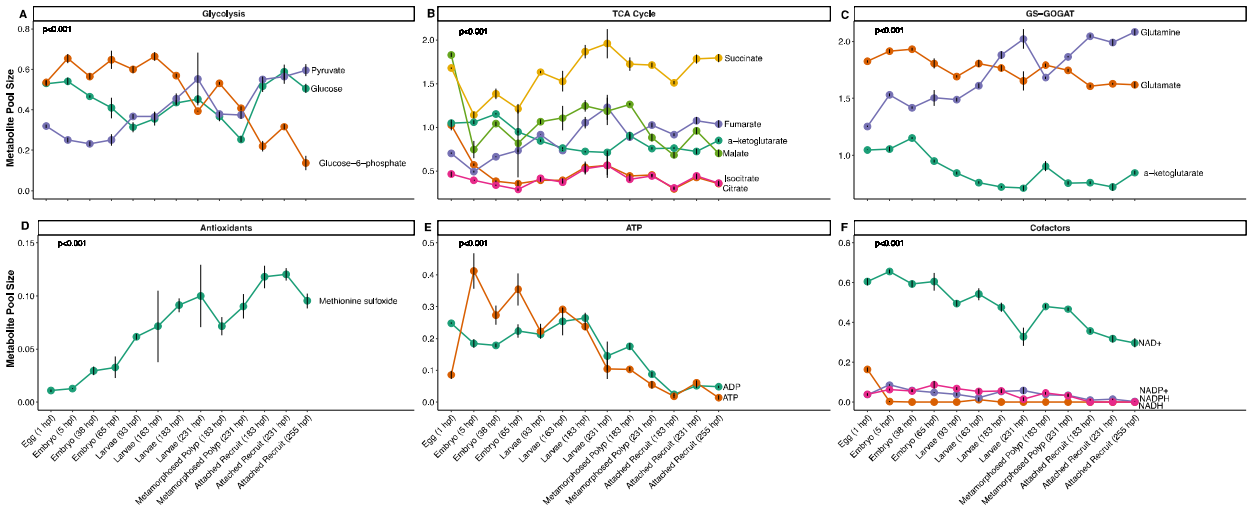

Fig 6. Pool size of metabolites involved in key metabolic pathways across *Montipora capitata* development. Metabolite pool size presented as mean ± standard error of log transformed median normalized ion intensity across life stages. Each metabolite is represented by a different color in each panel for visualization and labeled with metabolite identity. p-value indicates significance of life stage effects on gene expression (black indicates p<0.05). TCA indicates the tricarboxylic acid cycle; GS-GOGAT indicates the glutamine synthase-glutamine oxoglutarate aminotransferase pathway.

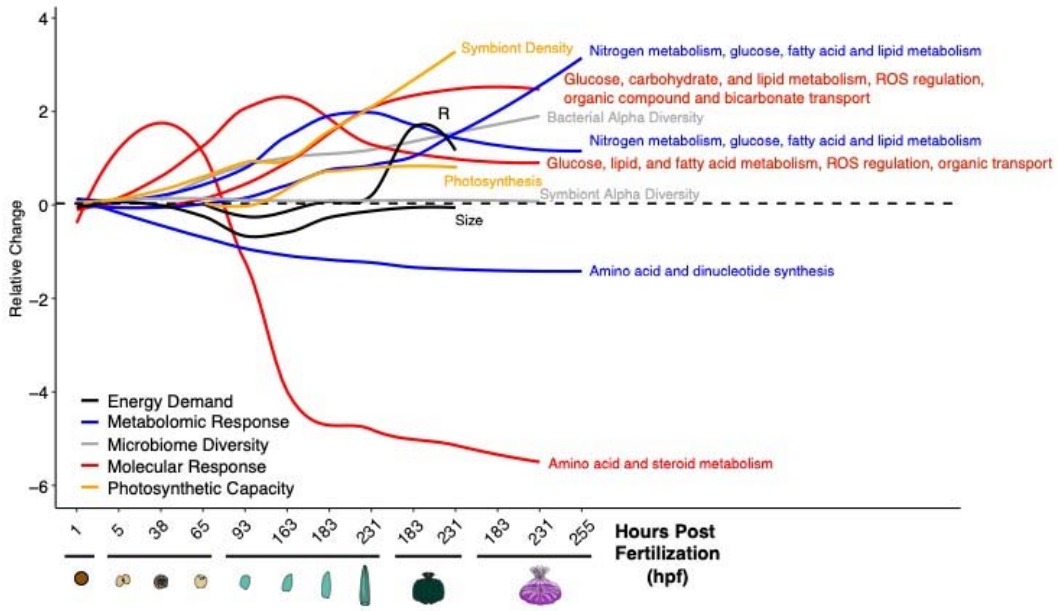

Fig 7. Relative change in response variables across a *Montipora capitata* developmental time series. Responses are characterized as energy demand (black; size and respiration [R]), metabolomic responses (blue; metabolomic ontogenetic patterns with key functional enrichment terms), molecular responses (red; gene expression ontogenetic patterns with key functional enrichment terms), microbiome diversity (gray; Symbiodiniaceae ITS2 alpha diversity and bacterial 16S alpha diversity), and photosynthetic capacity (orange; gross photosynthesis [“photosynthesis”] and symbiont density). Loess lines were plotted to indicate trends across life stages. Dashed line indicates a relative change of 0. Relative change calculated from the earliest available life stage in each data set. ROS = reactive oxygen species.